Nuclear Physics **A524** (1991) 228–250
North-Holland

THE ^{24}Mg(^{3}He, t)^{24}Al REACTION AND $L=1$ GIANT RESONANCE SYSTEMATICS USING AN EFFECTIVE ^{3}He–n INTERACTION AT 27 MeV/NUCLEON

M.B. GREENFIELD[1]

Physics Department, The Florida A&M University, Tallahassee, Florida, USA

S. BRANDENBURG, A.G. DRENTJE, P. GRASDIJK[2], H. RIEZEBOS[3], S.Y. VAN DER WERF and A. VAN DER WOUDE

Kernfysisch Versneller Instituut, 9747 AA Groningen, The Netherlands

M.N. HARAKEH and W.A. STERRENBURG

Faculteit der Natuurkunde en Sterrenkunde, Vrije Universiteit, Postbus 7161, 1007 MC Amsterdam, The Netherlands

B.A. BROWN

Cyclotron Laboratory, Michigan State University, East Lansing, MI 48824, USA

Received 21 June 1990
(Revised 28 September 1990)

Abstract: Differential cross sections from the ^{24}Mg(^{3}He, t)^{24}Al reaction have been measured from 0 to 32° in the laboratory system. DWBA calculations using an effective projectile-nucleon interaction are compared with the data to verify the applicability of such an approach as well as to deduce spectroscopic information. By employing DWBA in conjunction with transition amplitudes obtained from realistic microscopic wave functions, J^{π} assignments could be made. Strength normalizations for all observed transitions to positive-parity $T=1$ final states of ^{24}Al are given.

Localized $\Delta L=1$ strength around 10 MeV in excitation energy contains most of the expected isovector giant dipole resonance (GDR) and the magnetic quadrupole resonance (MQR) strengths with systematics that are consistent with those for most light, self-conjugate nuclei. A comparison with Coulomb-energy shifted (γ, n) data assists in locating the GDR analog. The isovector 0^{-} strength is not directly observed, but the total expected $\Delta L=1$, $\Delta S=1$ cross section is found in the broad collective "bump" at about 10 MeV and in a number of lower-lying states of negative parity.

E

NUCLEAR REACTIONS ^{24}Mg(^{3}He, t), $E=81$ MeV; measured $\sigma(E_t, \vartheta_t)$. ^{24}Al deduced levels, L, J, π. DWBA analysis, effective ^{3}He-n force, shell-model form factors. ^{12}C, ^{16}O, ^{24}Mg, ^{28}Si(^{3}He, t), $E=81$ MeV; ^{32}S(^{3}He, t), $E=73$ MeV; ^{40}Ca(^{3}He, t), $E=75$ MeV, measured $\sigma(E_t, \vartheta_t=0°)$, ^{12}N, ^{16}F, ^{24}Al, ^{28}P, ^{32}Cl, ^{40}Sc deduced isovector giant resonances.

[1] Present address: International Christian University, Mitaka-shi, Tokyo, Japan.
[2] Present address: PTT, Groningen, The Netherlands.
[3] Present address: Gasunie, Groningen, The Netherlands.

1. Introduction

Charge exchange reactions have become increasingly useful in investigating nuclear structure since the (p, n) [refs. [1-4])] and (^{3}He, t) [ref. [5])] reactions have been used as investigative tools for studying the isobaric analog resonance (IAR or IAS) in nuclei. The exploration of isovector spin resonances in 1975 via the (^{3}He, t) reaction [6]) and later in the (p, n) reaction [7-9]) led to the clear identification of the Gamow-Teller resonance (GTR). However as a result of these experiments it was found that about 40% of the $3(N-Z)$ sum-rule for Gamow-Teller strength [10]) seems to be missing. The nature of the mechanism for the depletion of this GT strength is not well established yet.

Shortly after the Gamow-Teller resonance was observed, isovector spin resonances, in which the orbital as well as spin angular momentum change by one unit, were observed in (p, n) [refs. [9,11-13])] and (^{3}He, t) [refs. [14-18])] experiments. When starting from a 0^+ ground state, an $L=1$ and $S=1$ transfer may couple to J^π of 0^-, 1^- and 2^-. This makes it difficult to resolve $\Delta L=1$ resonances into their different J^π components. Auerbach and Klein [19]) and Bertsch *et al.* [20]) have calculated strength distributions for such transitions in ^{90}Zr and found them to be fragmented, with centroids increasing in excitation energy for decreasing J^π. Furthermore the non-spin-flip analog of the giant dipole (1^-, $\Delta L=1$, $\Delta S=0$) is difficult to disentangle from the spin-flip component.

In the (^{3}He, t$\bar{p}$) reaction Sterrenburg *et al.* [16-18]) investigated these resonances in ^{12}N and ^{16}F and studied their decay into low-lying neutron hole states in ^{11}C and ^{15}O, respectively.

The energy dependence of the spin-isospin-dependent terms in the nucleon-nucleon interaction influences the choice of the energy per nucleon at which it is useful to observe isovector-spin resonances. In fact, the energy dependence of the excitation of spin resonances via charge-exchange interactions results from the energy dependence of the $V_{\sigma\tau}$ and $V_{T\tau}$ components of the nucleon-nucleon interaction. This energy dependence has been used to identify spin-flip strength [11]) and is being employed in resolving spin-flip from non-spin-flip components of the giant dipole resonance observed via (p, n) reactions [21]).

The (^{3}He, t) reaction has certain experimental advantages over other charge exchange reactions. The ejectile triton may be detected in a magnetic spectrograph with good energy resolution (in this case about 70 keV). The energy resolution of the (p, n) or heavy ion charge-exchange reactions, involving neutron detection in the former case and heavy ions in the latter, is typically much poorer. The disadvantage of the (^{3}He, t) reaction in comparison with the (p, n) reaction is the more complex reaction mechanism. Multi-step reaction processes should be considered for charge exchange reactions in general and the (^{3}He, t) reaction in particular [22]). It has, however, been shown that the (^{3}He, t) reaction at 27 MeV/nucleon may to a reasonable extent be approached as a one-step, direct reaction process, using an effective ^{3}He-n interaction [23]). The advantage of the high resolution that can be

achieved with the (^{3}He, t) reaction is apparent in fig. 1 which compares a $^{12}C(p, n)^{12}N$ spectrum [24,25]) at an incident energy of 160 MeV with a $^{12}C(^{3}He, t)^{12}N$ spectrum at 81 MeV [ref. [16])]. The structures, now known to be the analogs of the isovector magnetic quadrupole ($E_x \approx 4.2$ MeV) and the giant dipole ($E_x \approx 7$ MeV) resonances, are observed in both spectra. The similarity between the two spectra seems puzzling at first sight because the (p, n) reaction is known to be largely dominated by the real part of the $\sigma\tau$ force for all $\Delta L = 1$ excitations [25]), while for the (^{3}He, t) reaction the cross sections of the 2^- states are dominated by the tensor force [16-18]) and that of the giant dipole analog by the V_τ force. We shall come back to this point in sect. 4, which deals with the systematics of the $\Delta L = 1$ resonances.

By relating 0° (p, n) cross sections to B(GT) values, Anderson *et al.* [26]) searched for the expected GT strength by investigating the (p, n) reaction on targets of ^{12}C through ^{48}Ca, inclusive of ^{24}Mg. Substantial quenching of isovector spin-flip strength

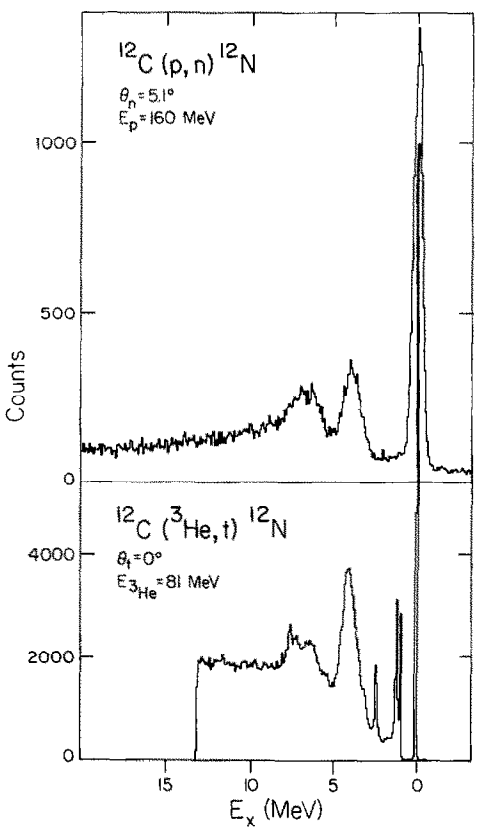

Fig. 1. $^{12}C(p, n)$ and $^{12}C(^{3}He, t)$ spectra at 160 and 81 MeV incident energy, respectively, displayed on a common excitation energy scale.

in the low excitation energy region has been observed in both (e, e') [refs. [27,28])] and (p, p') [refs. [29-32])], measurements of 1^+ transitions.

From a survey of all beta decay in the sd shell, Brown and Wildenthal [33,34]) find a uniform quenching of experimental decay rates as compared to extensive shell-model calculations. This quenching has been attributed to core polarization, to mesonic exchange currents leading to Δ-hole excitations and to mesonic exchange such as one-pion exchange and pionic-pair diagrams [34-36]).

In this work, by employing the (^{3}He, t) reaction with a higher resolution than in previous studies of ^{24}Al, we hope to determine whether previously unresolved 1^+ states may account for the missing strength. Furthermore, we will study the systematics of the isovector $\Delta L = 1$ resonances and investigate whether their collectivity and specific excitation remain for targets heavier than ^{12}C and ^{16}O.

A successful parametrization of the ^{3}He-n force at 10 MeV/nucleon has been given by Schaeffer [37]). The effective interaction used in this work [23]) is also a ^{3}He-n force with the same parametrization as used by Schaeffer. However, since the nucleon-nucleon interaction is energy dependent [38-40]), the ^{3}He-n potential was phenomenologically renormalized to describe the interaction at 27 MeV/nucleon [ref. [23])] by fitting the absolute cross sections and shapes of angular distributions of a large number of transitions on target nuclei ranging from ^{12}C to ^{90}Zr. This was achieved by ensuring the following conditions:

(i) The V_τ portion of the interaction must consistently fit observed isobaric analog states.

(ii) Stretched states for which one may assume pure particle-hole configurations must give consistent strengths for the tensor interaction. Spectroscopic factors for stretched spin configurations that are populated via the tensor interaction should agree with those obtained in (p, p'), (p, n) and (e, e') interaction studies [23]).

(iii) The $V_{\sigma\tau}$ along with the $V_{T\tau}$ terms should reasonably describe the 1^+ and 0^- states observed.

2. Experimental procedure

A momentum-analyzed 81 MeV ^{3}He beam from the Kernfysisch Versneller Instituut Cyclotron was transported to the spectrograph scattering chamber. The beam was scattered from targets of 0.79 mg/cm^2, isotopically enriched to 99.1% in ^{24}Mg. Targets were kept and transported in an oxygen-free environment to reduce contamination. Oxygen contamination, if present, would have been easily identifiable by the population of the dominant 2^- state at 0.424 MeV in ^{16}F.

Triton singles were detected in the QMG/2 magnetic spectrograph [41,42]). Optimal resolution of the spectrograph is about $\Delta E/E = 2 \times 10^{-4}$. For the case of 65 MeV tritons the overall resolution, due to different energy losses in the target of the ^{3}He and the triton, kinematic spread and aberrations due to saturation effects of the spectrograph magnetic field was about 70 keV. Tritons were detected in two 120 cm

position-sensitive focal-plane detectors mounted one behind the other and backed by a thin NE102 scintillator of the same length. This provided unambiguous identification of tritons in addition to the determination of their momenta. Details on this set-up have been reported elsewhere [43,44]).

Angular distributions from the $^{24}Mg(^{3}He, t)$ reaction were measured from 0 to 32° in the laboratory system with the QMG/2 spectrograph. For the 0° singles the beam was stopped with an internal Faraday cup, protruding into the vacuum chamber of the first dipole magnet of the QMG/2 spectrograph.

Sample data were taken on-line to monitor results. All data were stored on magnetic tape for later off-line analysis. This was accomplished with the program PAX [45]), a multi-parameter event mode data analyzer code.

Spectra at 0° have been taken on self-supporting targets of ^{12}C, ^{28}Si and ^{40}Ca, for ^{16}O on a Ta_2O_5 target and for ^{32}S on a target of sulphur sandwiched between gold foils. All targets had thicknesses between 0.5 and 1 mg/cm^2.

3. $^{24}Mg(^{3}He, t)^{24}Al$ data and analysis

3.1. PRESENTATION OF THE DATA

Fig. 2 shows a singles spectrum from the $^{24}Mg(^{3}He, t)^{24}Al$ reaction in comparison with a photonuclear (γ, n) spectrum (dashed line) [46,47]), shifted by the Coulomb energy difference (9.515 MeV) between the ^{24}Al ground state and its isobaric ($T = 1$) analog in ^{24}Mg. The correspondence with photonuclear work suggests that the bump around $E_x = 10$ MeV in the $(^{3}He, t)$ spectrum is the analog of the giant dipole resonance (GDR). A similar bump observed in the $(^{3}He, t)$ reaction on six targets of self-conjugate nuclei ranging from ^{12}C to ^{40}Ca at 25–27 MeV/nucleon exhibits corresponding similarities to photonuclear spectra shifted by Coulomb energies [18]) (see sect. 5). This correspondence has also been observed at 43 and 57 MeV/nucleon on targets from ^{12}C to ^{90}Zr [refs. [14,15])]. The clear observation of the GDR analog in the $(^{3}He, t)$ reaction shows that 1^- strength is excited at least in part by a non-spin-flip mechanism.

Figs. 3 and 4 show, respectively, the very forward and the more backward angle spectra of the $^{24}Mg(^{3}He, t)^{24}Al$ reaction for the energy region where sharp individual states are observed. Observed levels are labelled by numbers. In table 2 (see subsect. 3.3) the corresponding excitation energies, spin assignments and strengths are given.

3.2. MICROSCOPIC DWBA CALCULATIONS

In order to understand and interpret the experimental differential cross sections for observed low-lying states in ^{24}Al, microscopic one-step DWBA calculations were performed. The necessary ingredients for these calculations are the reaction mechanism, the available computer codes and the microscopic model wave functions. These will be discussed in short below.

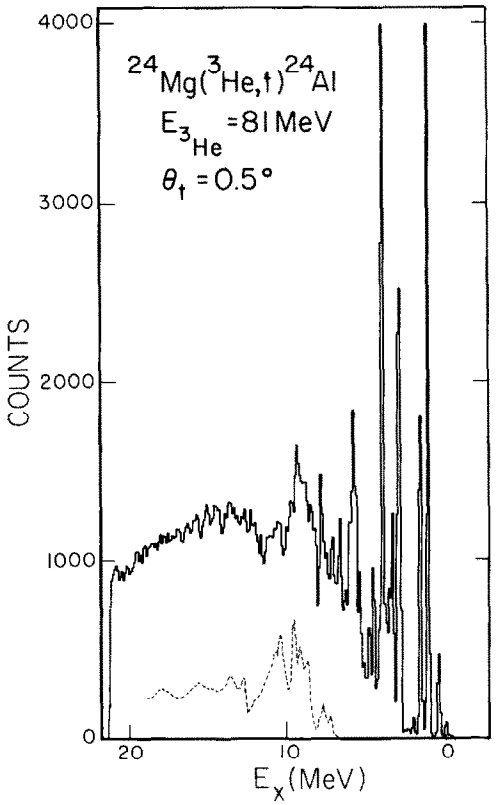

Fig. 2. $^{24}Mg(^{3}He, t)^{24}Al$ singles spectrum in comparison to the photonuclear cross section (dashed spectrum).

3.2.1. Reaction mechanism and effective interaction. The effective interaction is composed of the isospin-dependent components of the nucleon–nucleon interaction folded over the mass-3 system. Although, as mentioned, multi-step processes are not unexpected at 27 MeV/nucleon, consistent results may be obtained by assuming a direct, one-step transition induced by an effective interaction such as that given by Schaeffer [37]) after a term-by-term renormalization of the isospin-dependent potentials. The result of such a phenomenological renormalization of the Schaeffer force (new) is [23]):

$$V_{\text{eff}}(r) = \{V_\tau Y(r/R_\tau) + V_{\sigma\tau} Y(r/R_{\sigma\tau})(\boldsymbol{\sigma}_1 \cdot \boldsymbol{\sigma}_2) + V_{T\tau} r^2 Y(r/R_{T\tau}) S_{12}\}(\boldsymbol{\tau}_1 \cdot \boldsymbol{\tau}_2)\,,$$

where

$$V_\tau = 6.65 \text{ MeV}\,, \qquad V_{\sigma\tau} = -3.0 \text{ MeV}\,, \qquad V_{T\tau} = -6.50 \text{ MeV/fm}^2\,,$$

$$R_\tau = 1.415 \text{ fm}\,, \qquad R_{\sigma\tau} = 1.415 \text{ fm}\,, \qquad R_{T\tau} = 0.878 \text{ fm}\,.$$

3.2.2. DWBA formalism. The code we used to calculate angular distributions was DWBA82 by Raynal [48]). This is a full, finite-range, distorted-wave Born approximation, assuming a direct one-step mechanism. This code was used throughout except

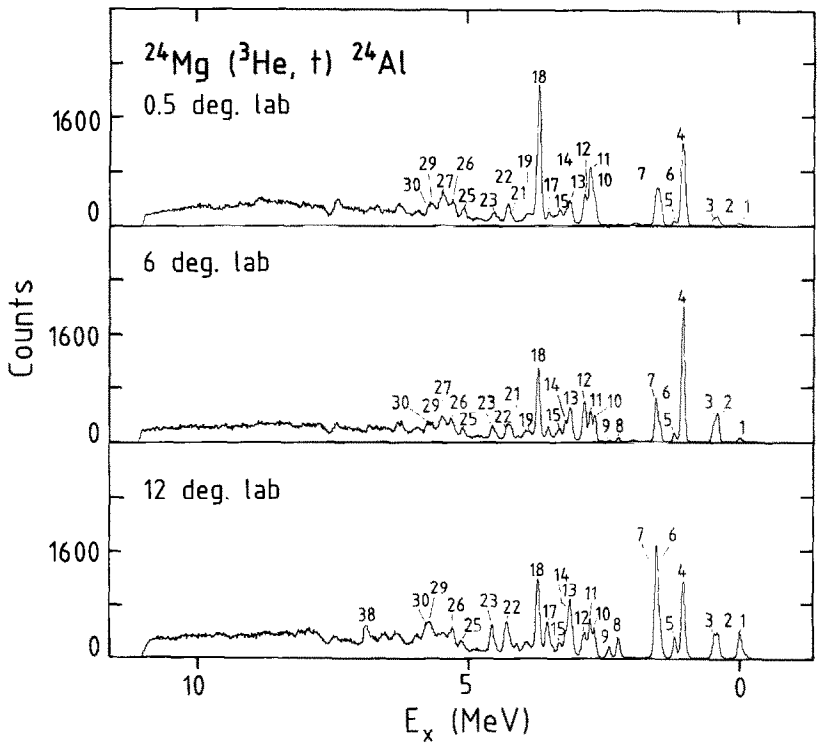

Fig. 3. $^{24}Mg(^{3}He, t)^{24}Al$ spectra taken at $\vartheta_{lab} = 0.5°$, 6°, 12°.

whenever the option of an unbound nucleon (proton) was needed. In those cases the equivalent, but slower, code DW81 [ref. [49])] was used. Both codes are updates of the original DWBA70 by Schaeffer and Raynal [50]).

3.2.3. Wave functions and particle-hole configurations. The transition densities in the microscopic DWBA calculations are based on the wave functions of Brown and Wildenthal [51]) which have been obtained in a full $0d_{5/2}$, $0d_{3/2}$, $1s_{1/2}$ (sd) basis using the "W" or "USD" interaction. These wave functions were then used to obtain the one-body transition densities (OBTD) between the ^{24}Mg $T = 0$ ground state and the positive-parity $T = 1$ states in ^{24}Al considered in the present work. The OBTD are available from the authors of ref. [51]). The predicted sd shell excitation energies agree quite well with the observed low-lying excitation energies of $T = 1$ states in the $A = 24$ triplet. This will be further discussed in subsect. 3.3.1.

Wave functions for final states of negative parity have been assumed to be pure $d_{5/2}$ hole $f_{7/2}$ particle. Although it is known that this basis is unrealistic, it is useful for the purpose of calculating the shapes as well as for establishing a measure for the magnitudes of the observed differential cross sections for negative-parity states.

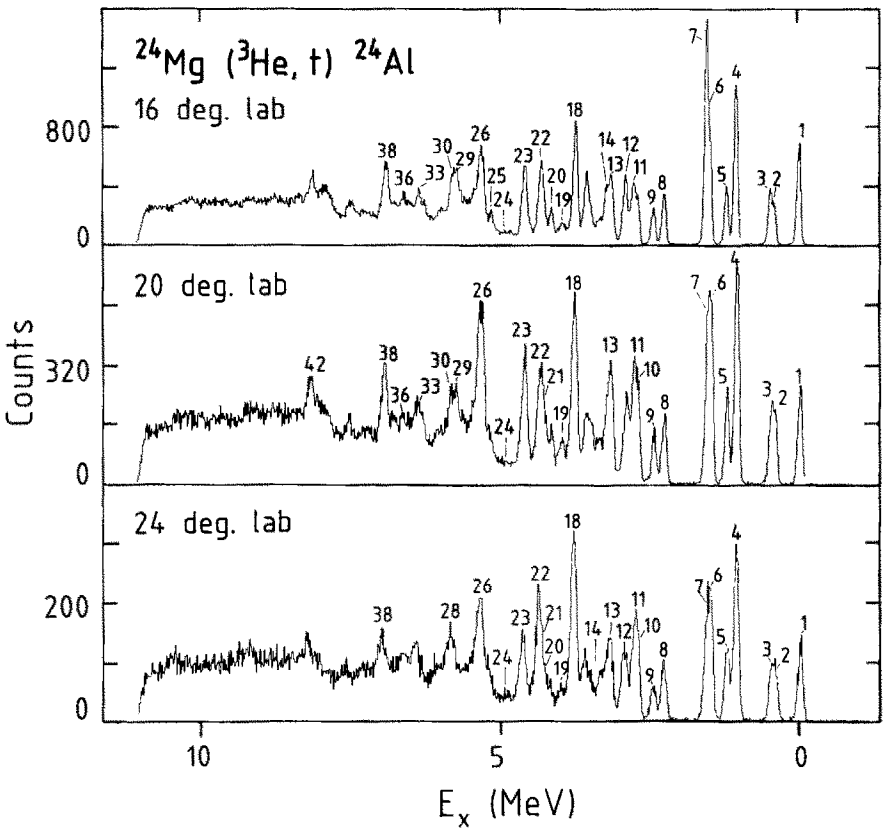

Fig. 4. $^{24}Mg(^{3}He, t)^{24}Al$ spectra taken at $\vartheta_{lab} = 16°, 20°, 24°$.

3.2.4. Optical-model parameters.

- ^{3}He optical-model parameters. A consistent family of volume-type optical-model parameters was determined by Grasdijk *et al.* [52]) from elastic scattering data on several nuclei ranging from mass 26 (^{26}Mg) to mass 58 (^{58}Ni). The parameters shown in table 1 and used in the analysis of the $^{24}Mg(^{3}He, t)^{24}Al$ reaction are those obtained for ^{26}Mg.

- Triton optical-model parameters. Triton optical-model parameters were determined by Grasdijk *et al.* [52]) as a global fit to isobaric analog states observed in the (^{3}He, t) reaction with fixed V_τ and the ^{3}He optical-model parameters shown in table 1. The real and imaginary well depths of the ^{3}He parameters were scaled by a common factor k. The cross sections at forward angles are insensitive to k, such that the search for V_τ and k could be decoupled. The best value for k obtained from a global fit to the IAS transitions on targets of ^{26}Mg, ^{42}Ca, ^{48}Ca, ^{58}Ni and ^{90}Zr was found to be 0.85. This value is used in all $^{24}Mg(^{3}He, t)^{24}Al$ calculations in this work.

TABLE 1

Optical-model parameters used in $^{24}Mg(^{3}He, t)^{24}Al$ calculations

	V_0 (MeV)	r_V (fm)	a_V (fm)	W_0 (MeV)	r_W (fm)	a_W (fm)	r_C (fm)
^{3}He	−112.0	1.14	0.85	−19.4	1.60	0.83	1.25
triton	−98.2	1.14	0.85	−16.5	1.60	0.83	1.25
n and p	adjust [a])	1.25	0.60			-	1.25

[a]) Neutron and proton real well depths were adjusted to fit their appropriate binding energy in the target and the residual nucleus. A Thomas spin-orbit strength $\lambda = 25$ was used.

3.3. COMPARISON OF DATA AND CALCULATIONS

In figs. 5-8 and 10 differential cross sections of transitions to states in ^{24}Al are compared with microscopic calculations using the computer codes DWBA82 of Raynal [48]) and DW81 of Comfort [49]). Although each J^{π} has in principle a characteristic angular distribution, in some cases differences are observed that reflect details of the nuclear structure. In particular it is difficult to distinguish a 1^{+} from a 2^{+} transition strictly on the basis of the shape of the calculated angular distribution.

While many $T = 1$ states in ^{24}Na and ^{24}Mg are known [53]), spin-parity assignments in ^{24}Al are restricted to the ground state (4^{+}) and the 1^{+} state at 0.439 MeV. Assignments made in this work for states in ^{24}Al rely primarily on shapes and magnitudes of calculated differential cross sections but predicted excitation energies and excitation energies of analog $T = 1$ states assist in tentative J^{π} determinations when the shapes of the angular distributions are not conclusive. Fig. 9 shows the $T = 1$ level scheme of the $A = 24$ triplet for states up to 4 MeV in excitation energy compared with the predicted level scheme of ref. [51]). Indicated correspondences between states in ^{24}Al, observed in the present work, with those in ^{24}Na and ^{24}Mg on the one hand and with the calculated levels on the other are suggested by the present analysis.

The angular distribution for the state at 5.47 MeV is also shown in fig. 10. Although reasonably well fitted by a stretched 6^{-} angular distribution, it is difficult to distinguish it clearly from a 5^{+} angular distribution. This state and other negative-parity states will be discussed below.

3.3.1. Positive-parity states. In figs. 5-8 differential cross sections for states in ^{24}Al, mostly of positive parity, are shown with corresponding DWBA calculations. In these figures the states have been grouped according to their spin, but in many cases second choices for the assignment have been indicated and unresolved groups have been analyzed with sums of theoretical curves.

In table 2 all levels observed are labelled with their peak numbers from figs. 3 and 4 and are matched up with theoretical counterparts in the manner described

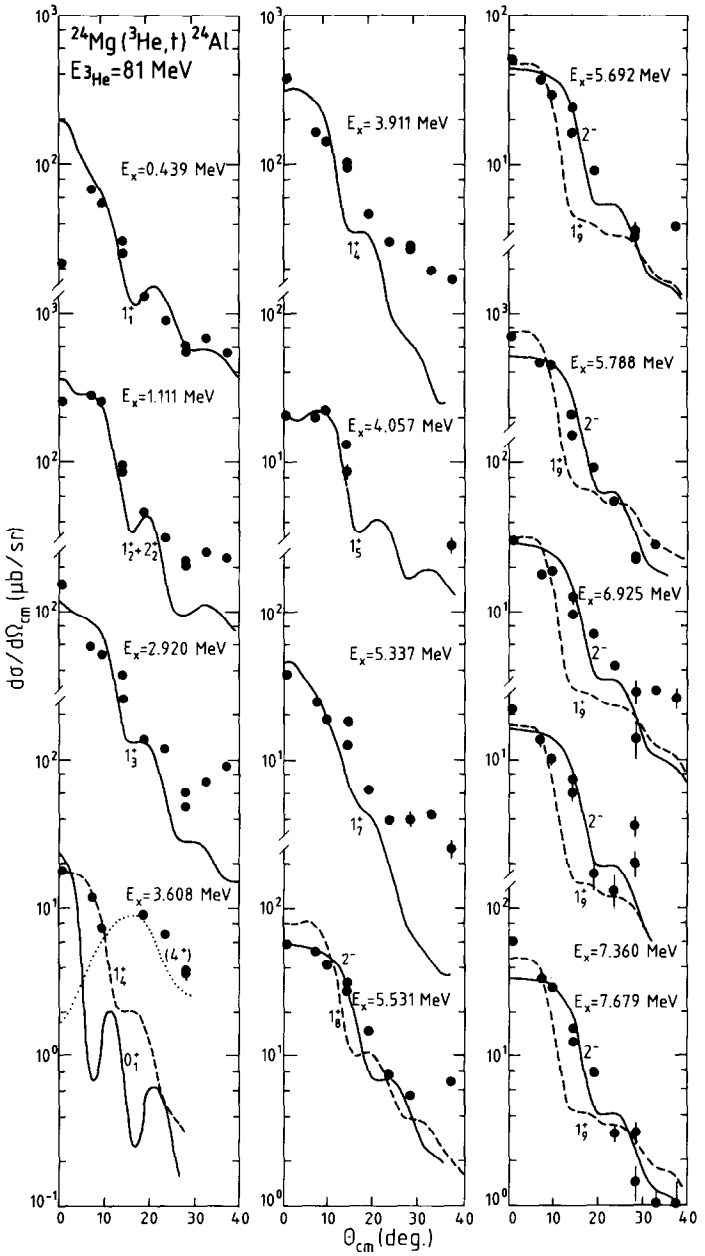

Fig. 5. Experimental and calculated differential cross sections for 1^+ and possible 2^- states identified in this work. The model wave functions on which these calculations are based are indicated in the same notation as in table 2.

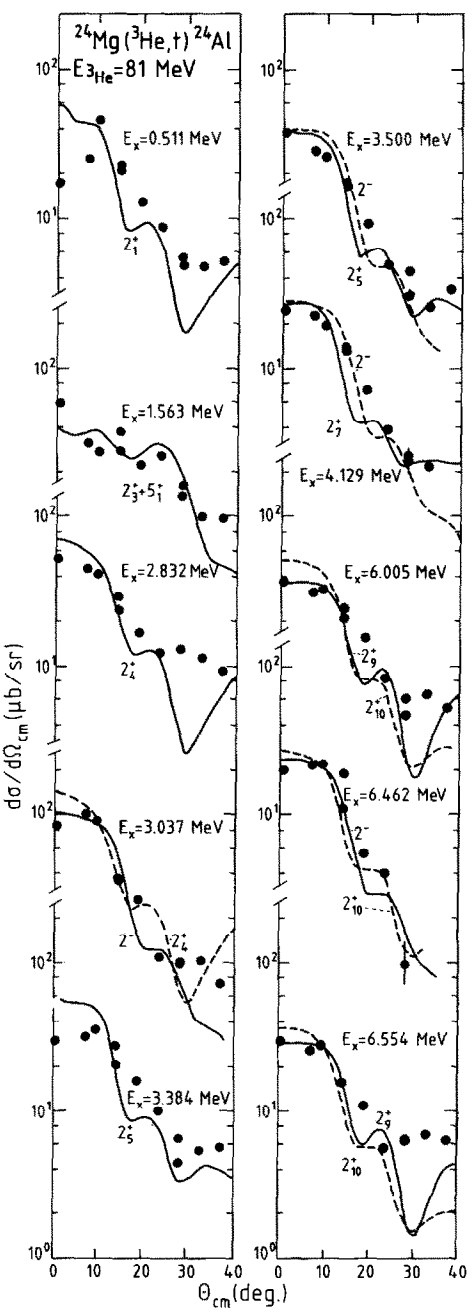

Fig. 6. Experimental and calculated differential cross sections for 2^+ states identified in this work. The model wave functions on which these calculations are based are indicated in the same notation as in table 2.

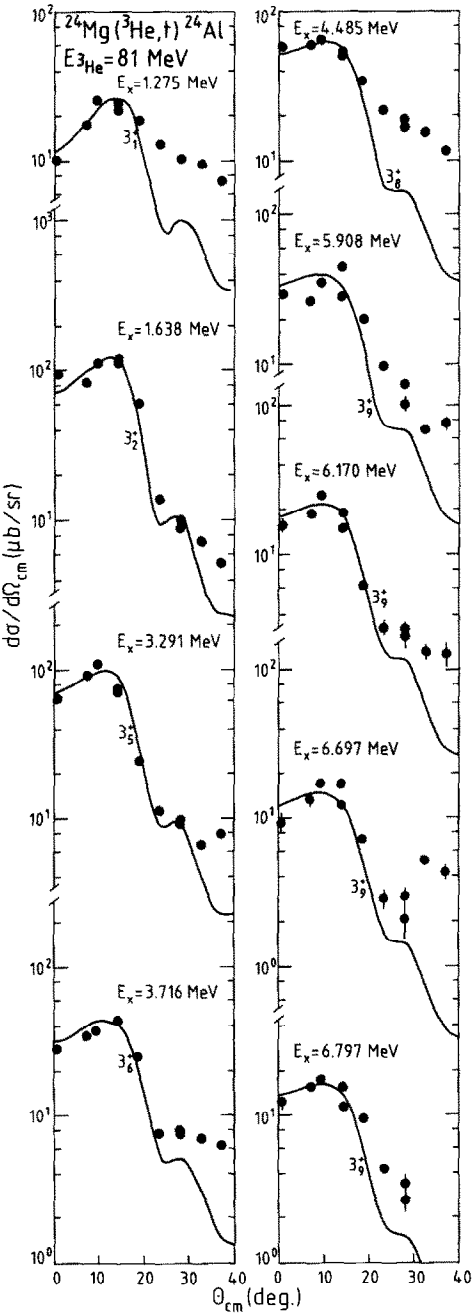

Fig. 7. Experimental and calculated differential cross sections for 3^+ states identified in this work. The model wave functions on which these calculations are based are indicated in the same notation as in table 2.

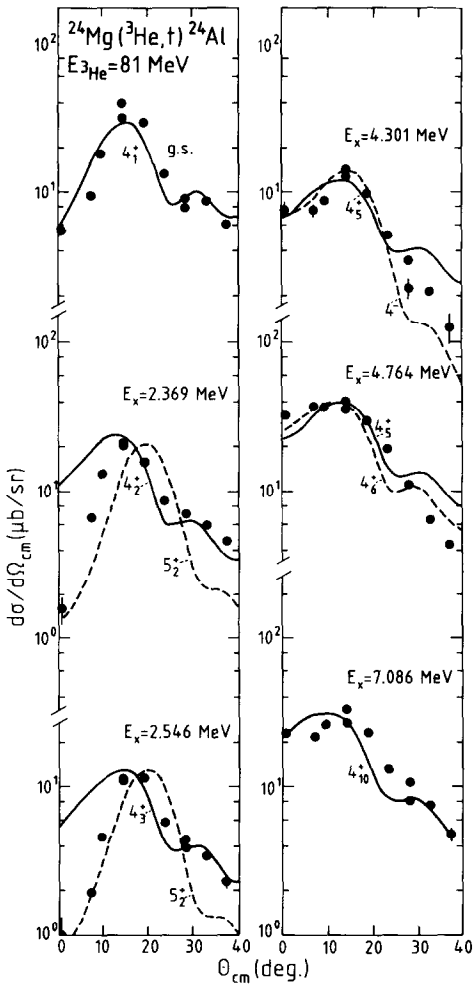

Fig. 8. Experimental and calculated differential cross sections for 4^+ states identified in this work. The model wave functions on which these calculations are based on indicated in the same notation as in table 2.

below. The subscripts 1, 2, 3, . . . , 10 attached to each J^π value designate the ordinal number of the theoretical sd-shell level for positive parity.

Although a precise one-to-one correspondence between predicted and observed levels is neither expected nor observed, this procedure is used for the sake of comparison. On the one hand the experiment does not always resolve closely spaced states and on the other hand there may be non-sd intruder levels of positive parity.

The group at $E_x = 1.12$ MeV has been shown to be a doublet of a state at 1.11 MeV and another at 1.13 MeV [ref. [54])]. Relying on the correspondence with the level ordering in ^{24}Na and ^{24}Mg and guided by the theoretical level scheme one infers

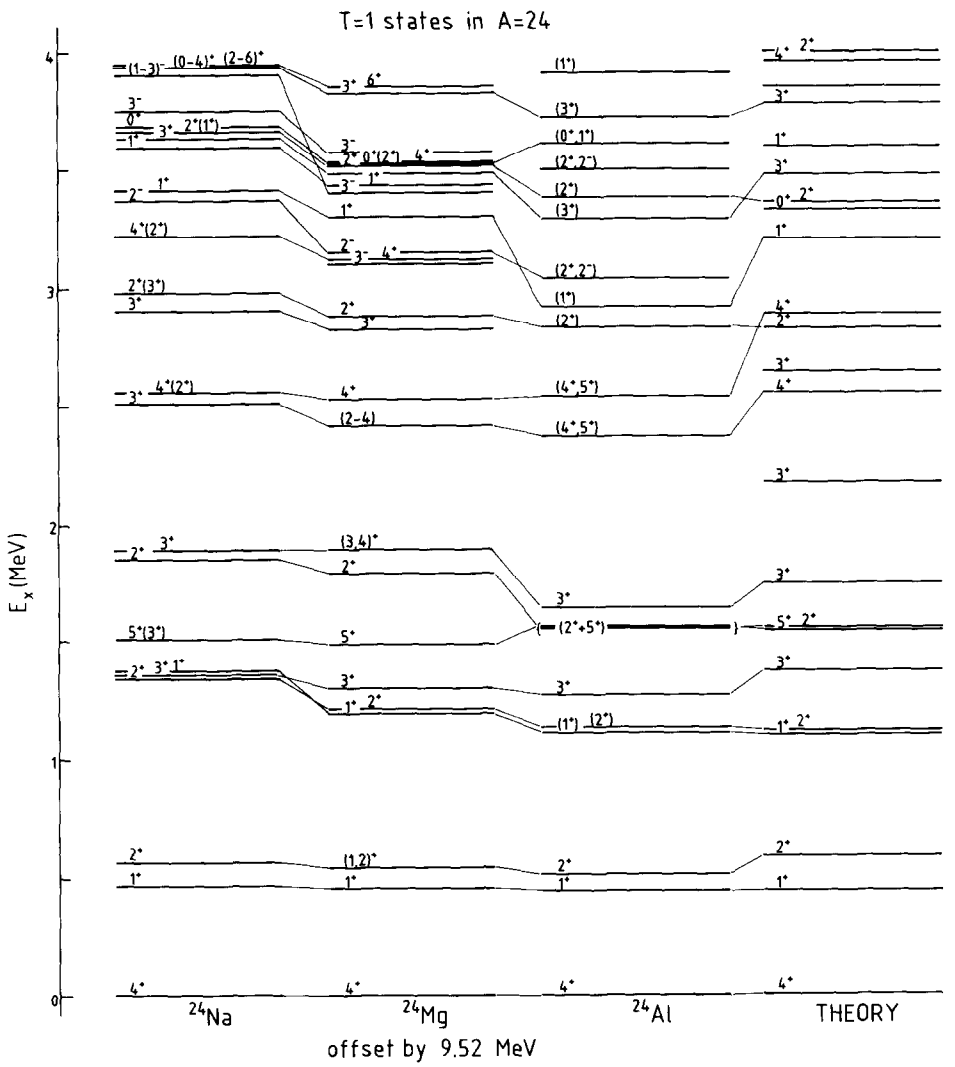

Fig. 9. $T = 1$ levels in the $A = 24$ triplet. Data on ^{24}Na and ^{24}Mg and the correspondences between them are from ref. [53]). The levels in ^{24}Al are from the present work. The level scheme in the right column shows the result of the shell-model calculation of ref. [51]). The correspondences of levels of ^{24}Al with analogs in ^{24}Na and ^{24}Mg and with the theoretical levels are from the present work.

that these must be a 1^+ state and a 2^+ state. Since the cross section for the 1_2^+ state is predicted to be much larger than that of the 2_2^+ state and the centroid energy is 1.111 MeV in our experiment we conclude that the lowest of the two must be the 1^+ state.

The relatively poor fit of the 2_3^+ model state to the group at 1.56 MeV seems to be due to the presence of the 5_1^+ state and the group has been analyzed assuming

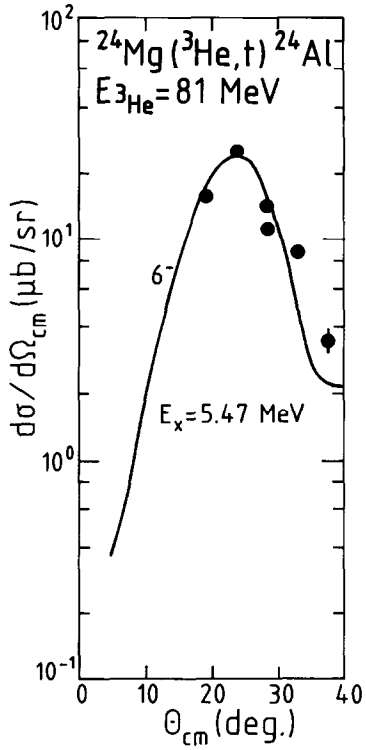

Fig. 10. Differential cross section and fit for the 6^- state at 5.47 MeV.

the presence of this doublet. For states above 3 MeV negative-parity states may be expected and an assignment of 2^- gives a better fit in some cases than do 1^+ or 2^+ assignments.

The spin assignment to 3^+ states is less ambiguous in general than to 1^+ and 2^+ states and fits are of good quality. The model states 3_3^+ and 3_4^+ are predicted to give very small cross sections and no corresponding candidates are observed experimentally in ^{24}Al. However, the states at $E_x = 2.90$ MeV in ^{24}Na and at $E_x =$ 12.339 MeV in ^{24}Mg [ref. [53])] correspond well with the theoretical 3_4^+ state.

The 5_2^+ state is predicted to lie above 5 MeV excitation energy. Therefore the states at 2.369 and 2.546 MeV are most probably 4^+ states, although 5^+ reproduces the differential cross sections better at forward angles. For states above 3 MeV a 4^- assignment is also possible.

3.3.2. Normalizations for positive-parity states. All of the above calculations shown in figs. 5–8 have been normalized to the data by factors $[(d\sigma/d\Omega)_{exp}/(d\sigma/d\Omega)_{calc}]$, the square roots of which, N, are given in table 2. Most of the fits could be normalized with factors N ranging from about 0.6 to 2.0. This agreement was observed previously with the Schaeffer force where the wave functions of Gillet and Vinh Mau [55]) or

TABLE 2

States observed in ^{24}Al via the $^{24}Mg(^{3}He, t)^{24}Al$ reaction. Spin assignments and normalization factors for the effective ^{3}He–n force

Peak number	E_x (MeV)	J^π	Model wave function [a]	Normalization [b]
1	0.000	4^+	4^+	8.5
2	0.439 ± 0.006	1^+	1_1^+	3.2
3	0.511 ± 0.004	2^+	2_1^+	2.2
4	1.111 ± 0.003	$\{1^+, 2^+\}$	$\{1_2^+, 2_2^+\}$	0.89
5	1.275 ± 0.005	3^+	3_1^+	0.81
6	1.563 ± 0.007	$\{(5^+), (2^+)\}$	$\{5_1^+, 2_3^+\}$	1.0, 2.2
7	1.638 ± 0.008	3^+	3_2^+	1.0
8	2.369 ± 0.004	$(4^+, 5^+)$	$4_2^+, 5_2^+$	4.4, 1.4
9	2.546 ± 0.007	$(4^+, 5^+)$	$4_3^+, 5_2^+$	2.4, 1.0
10	2.832 ± 0.006	2^+	2_4^+	3.3
11	2.920 ± 0.023	(1^+)	1_3^+	0.71
12	3.037 ± 0.016	(2^+)	$2_4^+, d_5^{-1}f_7$	4.6, 0.20
13	3.291 ± 0.012	3^+	3_5^+	1.4
14	3.384 ± 0.016	(2^+)	2_5^+	2.1
15	3.500 ± 0.019	$(2^+, 2^-)$	$2_5^+, d_5^{-1}f_7$	1.3, 0.13
16	3.608 ± 0.016	$(0^+, 1^+)$	$0_1^+, 1_4^+$	1.9, 0.76
17	3.716 ± 0.010	3^+	3_6^+	1.4
18	3.911 ± 0.006	(1^+)	1_4^+	3.2
19	4.057 ± 0.017	(1^+)	1_5^+	0.95
20	4.129 ± 0.024	$(2^+, 2^-)$	$2_7^+, d_5^{-1}f_7$	1.3, 0.10
21	4.301 ± 0.031	$(4^+, 4^-)$	$4_5^+, d_5^{-1}f_7$	1.8, 0.15
22	4.485 ± 0.010	3^+	3_8^+	1.2
23	4.764 ± 0.008	(4^+)	$4_5^+, 4_6^+$	3.3, 10.5
24	5.045 ± 0.33	-	no fit	
25	5.337 ± 0.010	(1^+)	1_7^+	2.2
26	5.470 ± 0.017	6^-	$d_5^{-1}f_7$	0.50
27	5.531 ± 0.019	$(1^+, 2^-)$	$1_8^+, d_5^{-1}f_7$	2.2, 0.15
28	5.614 ± 0.022	-	no fit	
29	5.692 ± 0.026	$(1^+, 2^-)$	$1_9^+, d_5^{-1}f_7$	3.2, 0.14
30	5.788 ± 0.034	$(1^+, 2^-)$	$1_9^+, d_5^{-1}f_7$	4.0, 0.44
31	5.908 ± 0.016	(3^+)	3_9^+	1.3
32	6.005 ± 0.014	(2^+)	$2_9^+, 2_{10}^+$	3.5, 2.1
33	6.170 ± 0.016	(3^+)	3_9^+	1.0
34	6.324 ± 0.048	-	no fit	
35	6.462 ± 0.024	$(2^+, 2^-)$	$2_{10}^+, d_5^{-1}f_7$	1.6, 0.10
36	6.554 ± 0.015	(2^+)	$2_9^+, 2_{10}^+$	3.3, 1.7
37	6.697 ± 0.019	(3^+)	3_9^+	0.83
38	6.797 ± 0.023	(3^+)	3_9^+	0.90
39	6.925 ± 0.032	$(1^+, 2^-)$	$1_9^+, d_5^{-1}f_7$	2.6, 0.11
40	7.086 ± 0.008	$(4^+, 4^-)$	4_{10}^+	17.6
41	7.360 ± 0.003	$(1^+, 2^-)$	$1_9^+, d_5^{-1}f_7$	1.8, 0.08
42	7.441 ± 0.018	-	no fit	
43	7.679 ± 0.020	$(1^+, 2^-)$	$1_9^+, d_5^{-1}f_7$	3.2, 0.12

[a] The model wave functions are based on the "W" or "USD" interaction of ref. [51]). For negative-parity states the simple configuration $1d_{5/2}^{-}1f_{7/2}$ was assumed.

[b] $N = [(d\sigma/d\Omega)_{exp}/(d\sigma/d\Omega)_{calc}]^{1/2}$.

Clark and Elliott [56]) were used to calculate transitions to final states of ^{12}N and ^{16}F [refs. [16,17])].

It was concluded in ref. [23]) that normalization factors for transitions to unnatural parity states are usually around unity and thus that differential cross sections are described in a quantitative way. This is found to be true in this work for the 3^+ states. For the 1^+ states it is true for some of the states with a notable exception for the fit of the 0.439 MeV state. We will come back to this later on. The normalization factors for 2^+ states average around 2 and for the 4^+ states this value is between 4 and 5. This effect was noted in ref. [23]) and was suggested to be indicative for a possible contribution of an $L \cdot S$ term in the effective force. It has been shown that such a spin-orbit term spoils the fits to isobaric analog transitions, but greatly improves the fits to the shapes of higher spin states. It would, however, need a strength roughly proportional to the square of the final spin in order to match the magnitude of the cross sections. Because of this inconsistency we chose to leave it out of the effective force used in the present analysis. It should, however, be noted that such a phenomenologically scaled $L \cdot S$ contribution would improve the fits at forward angles for the 4^+ states, thus strengthening the 4^+ assignments of the states at 2.369 and 2.546 MeV.

The fact that normalization factors for natural parity states need a scaling roughly proportional to the square of the angular momentum transfer suggests that possibly a $L \cdot L$ term is needed in the effective interaction. At present the available computer codes do not provide this option*.

The angular distribution of the 1^+ state at 0.439 MeV exhibits an unexpected strong dip at 0°. This might be due to interference between dominant terms in the model wave functions ($2s_{1/2}$, $1d_{3/2}$ and $1d_{5/2}$, $1d_{3/2}$ for example). Sample calculations attempting to explain this effect have, however, been unsuccessful in reproducing this effect.

In previous $^{24}Mg(p, n)^{24}Al$ measurements [26]), 0° 1^+ cross sections were measured for the purpose of separating current and spin contributions to Gamow-Teller transitions. An earlier study by Berg *et al.* [57]) compared the angle-integrated (p, n) cross sections at 35 MeV with $B(GT)$ values obtained from inelastic electron-scattering experiments for the analog transitions. Both analyses, differing only in whether an overall normalization factor was used or not, showed reasonably good agreement between the (p, n) cross sections and $B(GT)$ values. Anderson *et al.* [26]) observed 0^+ to 1^+ transitions around 0.4, 1.1 and 3.1 MeV in excitation. In the present work further 1^+ strength was tentatively identified up to 7 MeV. This observation of additional 1^+ states can, however, not be used to draw any conclusions on the question of the missing Gamow-Teller strength. We can conclude that most of the cross section predicted for 1^+ states below 7 MeV is seen, but this cross section is dominated by the tensor component of the effective force. The $V_{\sigma\tau}$ term is important only at very forward angles and any conclusion on Gamow-Teller strength would

* Note added in proof: the very recently released update DWBA90 of J. Raynal allows as new features $L \cdot L$ and $(L \cdot S)^2$ terms.

have to be based on 0° cross sections. The calculated sum of the 0° cross sections for 1^+ states below 8 MeV in excitation energy is 0.90 mb/sr. This is the sum for the first ten model states. Experimentally we find 0.80 mb/sr on states assigned 1^+ below 5.5 MeV. Above that energy assignments of 2^- and 1^+ are in competition, but another 0.1 or 0.2 mb/sr might well reside on 1^+ states. It appears therefore that we identify in the present work most of the low-lying cross section that is theoretically predicted for 1^+ strength.

3.3.3. Negative-parity states. A full shell-model calculation based not only on 1f and 2p particles and 1d and 2s holes but also on 1d and 2s particles and 1p holes was not performed. Most strength associated with such configurations is expected to lie above 7 MeV in excitation energy. The few states that could be of negative parity, either on the basis of their angular distributions or by a possible association with an analog in ^{24}Na or ^{24}Mg have been analyzed with a single $(d_{5/2}^{-1}f_{7/2})$ component for the sake of obtaining a quantitative standard. However, a calculation including all $1\hbar\omega$ $\Delta L = 1$ single-particle transitions was performed in order to obtain an estimate for the total expected cross sections to the $(0^-, 1^-, 2^-)$ bump around 10 MeV (table 3).

For ^{12}C and $^{16}O(^{3}He, t)$ reactions, magnetic quadrupole strength has been observed as a collective excitation whereas in heavier targets it seems to be fragmented. For ^{24}Mg several possible 2^- fragments down to excitation energies as low as 3 MeV are observed. Their summed cross section constitutes, however, not more than some 20% of the expected strength for the $(d_{5/2}^{-1}f_{7/2})$ configuration alone. We will discuss the issue of the $(0^-, 1^-, 2^-)$ strength observed at higher excitation energies in sect. 4 in the context of the systematics of this strength for self-conjugate nuclei.

TABLE 3

Predicted [a]) $\Delta L = 1$ zero degree cross sections to all 1p-1h configurations within a $1\hbar\omega$ space and experimental cross sections observed [b]) in the $(^{3}He, t)$ reaction on targets of light self-conjugate nuclei

Target	0^-	1^-	2^-	$\Delta L = 1$ (calc)	$\Delta L = 1$ (obs)
^{12}C	0.17	1.34	4.39	5.90	6.0 ± 1.0
^{16}O	0.19	0.85	7.19	8.23	7.4 ± 1.2
^{24}Mg	0.24	0.57	5.90	6.71	6.4 ± 1.1
^{28}Si	0.30	0.64	6.14	7.08	9.8 ± 1.3
^{32}S	0.09	0.32	6.53	6.94	6.4 ± 1.1
^{40}Ca	0.60	0.70	6.52	7.82	9.9 ± 2.0

[a]) Calculation using the effective ^{3}He-n force of ref. [23]) assuming $1\hbar\omega$ $\Delta L = 1$ transitions from the closed-core configurations ^{12}C: $(p_{3/2})^8$, ^{16}O: $(p_{1/2})^4$, ^{28}Si: $(d_{5/2})^{12}$, ^{32}S: $(s_{1/2})^4$ and ^{40}Ca: $(d_{3/2})^8$. A $(d_{5/2})^8$ configuration was adopted for ^{24}Mg (g.s.). Adopted Q-values are −22 MeV (2^-), −25 MeV (1^-) and −28 MeV (0^-).

[b]) All observed cross sections above the breakup-transfer background in the energy region $Q \leq -18$ MeV and $\Delta L = 1$ transfer in individual peaks or clusters identified for $Q \geq -18$ MeV.

The most interesting of the negative-parity states in the low excitation energy region is the 6^- state at 5.47 MeV. A simple wave function for a stretched state at 5.47 MeV may be assumed to be a pure $1\hbar\omega$ excitation of a $d_{5/2}^{-5}$ hole configuration coupled to an $f_{7/2}$ particle excited from a $d_{5/2}^{-4}$ ground state. The calculated cross section for such a state, like the experimental angular distribution shown, peaks at about 23° (see fig. 10). The fit is good and provides a good test for the tensor part of the effective interaction through which the stretched state is excited. The quenching factor, adopting the same simple wave function and the same bound-state nucleon geometrical parameters is found to be 0.38 from (p, p') and 0.41 from (e, e') [ref. [23])]. This is indicative of the degree to which the 6^- strength is fragmented. The remaining cross section is expected to be moved to higher excitation energy.

4. $\Delta L = 1$ giant resonance systematics

In fig. 11 the (^{3}He, t) spectra taken at 0° on ^{12}C, ^{16}O, ^{24}Mg, ^{28}Si, ^{32}S and ^{40}Ca are compared with corresponding photo-absorption spectra [46,47,58]). The choice of 0° as the angle for which to present the spectra is based on the fact that the 0^- and 2^- angular distributions are peaked at this angle, while those for the 1^- states are only slightly smaller than they are at their first maximum around 6°. Relevant sample angular distributions may be found in refs. [16–18]) and in figs. 5 and 6 of the present work.

In the (γ, n) spectra almost all of the strength is observed on the isovector giant dipole resonance (GDR) which goes via $\Delta L = 1$, $\Delta S = 0$ transfer. By comparing the photo-absorption spectra of the target nucleus with the corresponding (^{3}He, t) spectra, one may identify the analog of the GDR in the final nucleus. In all of the self-conjugate nuclei shown in fig. 11, except ^{32}S, where a photo-absorption spectrum is not available, there is remarkable agreement between the two spectra with regard to both location and shape of the GDR. The shaded areas represent the estimated contribution from the breakup-transfer reaction. In this process the kinetic energy available in the outgoing channel is shared between the triton and a spectator-proton and gives rise to a continuous triton spectrum with a shape that is essentially given by the momentum distribution of the spectator-proton inside the ^{3}He projectile superimposed on the beam velocity and the three-body phase space of the reaction [59,60]). The shape of the spectrum is found to be reliably reproduced by this model [17]). Absolute cross sections invoke renormalization factors that include the effects of distortion and absorption [60]). Matching the breakup-transfer contribution to the observed spectrum at the lowest recorded triton energies yields an upper limit for the breakup-transfer contribution and therefore a lower limit for the giant resonances cross sections.

The Q-value for the analog of the GDR can be estimated from the GDR excitation energy systematics [61]) in the parent nucleus (A, Z) and the Coulomb energy difference as

$$Q(\mathrm{GDR}) = -31.2A^{-1/3} - 20.6A^{-1/6} - 0.70(2Z+1)(1-0.76Z^{-2/3})A^{-1/3} + 0.764\ \mathrm{MeV}.$$

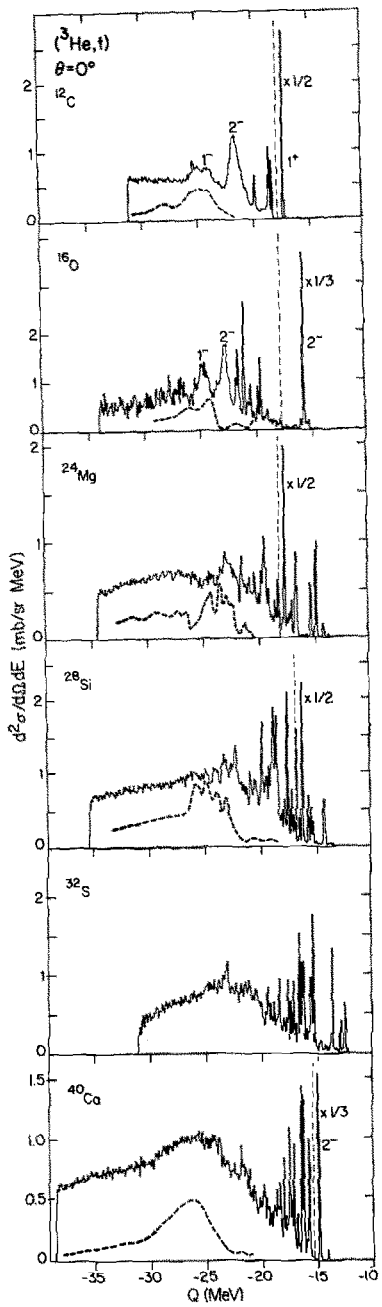

Fig. 11. ^{12}C, ^{16}O, ^{24}Mg, ^{28}Si, ^{32}S, ^{40}Ca (^{3}He, t) spectra taken at $\vartheta_{lab} = 0°$. The dashed lines represent the photo-nuclear (γ, n) spectra shifted by the excitation energy of the lowest $T = 1$ state in the target nucleus. The shaded areas correspond to the breakup-transfer cross section (see text).

The decrease of the first two terms with mass is nearly exactly counterbalanced by the increase of the Coulomb energy difference (third term), resulting in a predicted mean Q-value of -27 MeV for the GDR analog for all nuclei displayed in fig. 11. Experimentally the peak in the spectrum associated with the GDR lies around -25 MeV. The centroid energy of the magnetic quadrupole resonance (2^-) is around -22 MeV and the 0^- is expected around -28 MeV [refs. [16-18])]. We adopt these Q-values in a calculation of the total cross section for all $\Delta L = 1$ transitions within a $1\hbar\omega$ space. For each spin-parity class $J^\pi = 0^-$, 1^- and 2^-, cross sections were calculated for all single $1\hbar\omega$ one-particle-one-hole configurations relative to an adopted closed core configuration (see table 3) and were then added incoherently.

The results are listed in table 3 and compared with the experimental cross sections obtained by integrating the spectra above the assumed breakup-transfer background from $Q = -18$ MeV downwards and the cross section in peaks or clusters at less negative Q-values identified tentatively as $L = 1$ transfers. It has to be noted here that the agreement is remarkable: all the predicted cross section seems to be accounted for by the calculation despite the fact that the breakup-transfer contribution has been taken maximal and thus the observed cross section associated with the $\Delta L = 1$ resonances as minimal.

A notable feature of these calculated cross sections is the dominance of the 2^- component. The 0^- component is predicted to be small and its main cross section is expected at higher excitation energies. Also the 1^- component, part of which is observed in the lighter nuclei and can be identified through its correspondence with the photonuclear spectra is predicted to be small as compared to the 2^- component. Thus it appears that the 2^- strength peaks at a Q-value around -22 MeV but in addition has a strong tail that extends towards higher energies.

It remains to investigate to which extent the (^{3}He, t) is selective for the excitation of the analog of the giant dipole resonance which is characterized by $\Delta L = 1$, $\Delta S = 0$. This selectivity is suggested by the resemblance with photo-nuclear spectra. In sect. 1 it was shown that the spectra of the (^{3}He, t) and the (p, n) reactions taken on ^{12}C also exhibit a striking similarity. We take ^{12}C as a case study to investigate the origin of this resemblance, using the wave functions of Gillet and Vinh-Mau [55]). These wave functions have been used in ref. [16]) in an analysis of the (^{3}He, t) reaction. They correctly reproduce the observations that the largest fragment of strength for the $[\sigma \times rY_1 t_-; 2^-]$ operator, which is represented by the 2^-_2 model state, comes around $E_x = 4$ MeV, while most of the $[rY_1 t_-; 1^-]$ strength falls around $E_x = 7$ MeV. This latter strength resides on the 1^-_2 model state. Higher-lying 1^- model states carry the main part of the $[\sigma \times rY_1 t_-; 1^-]$ spin-flip strength. In the (^{3}He, t) reaction the 2^- states are fully dominated by the tensor component of the effective force and the 2^-_2 state has the largest cross section. In the (p, n) reaction at 160 MeV this state is excited mostly by the real part of the $\sigma\tau$ force. The 1^-_2 state is dominated by the V_τ force in the (^{3}He, t) reaction and also has a cross section which is an order of magnitude larger than those of the other 1^- model states. Also in the (p, n) reaction for the 1^-_2 state the V_τ contribution is the most important, just slightly larger than

that of the $\sigma\tau$ component. Unlike in the (^{3}He, t) reaction the cross sections of the higher 1^- and 2^- model states are not smaller here than that of the 1_2^- state, but are of comparable magnitude.

With the help of the unbound-state subroutine, as for example used in the program DW81 [ref. [49])], one finds that the 2_2^- state has a half-width of about 0.8 MeV while that of the 1_2^- is about 3.0 MeV. The widths of the higher-lying states are significantly larger, in the order of 10 MeV. Thus the fact that the cross section in the 1_2^- model state, which represents most of the non-spin-flip dipole strength, is also pronounced in the (p, n) reaction (see fig. 1) is caused mostly by the smaller width of this state. In the (^{3}He, t) reaction it is caused in addition by its prominent cross section.

The situation with regard to the selectivity of the (^{3}He, t) reaction for the non-spin-flip strength on 1^- states is similar for the other self-conjugate targets investigated in this work: the analog of the GDR is excited strongly in the first place and secondly it happens to lie in an excitation energy region where a single particle-hole state still has a sufficiently small width to make it stand out as compared to higher-lying states.

5. Summary and conclusions

Recent success in establishing an effective ^{3}He-n interaction for the (^{3}He, t) reaction along with significantly better energy resolution make the (^{3}He, t) reaction a viable charge exchange reaction. A one-step, direct reaction model based on a phenomenological renormalization of the Schaeffer force provides a useful approach for the (^{3}He, t) reaction at 27 MeV/nucleon. Using this approach makes the (^{3}He, t) reaction a useful spectroscopic tool. Spin-parity assignments, based upon comparison with DWBA using microscopic transition densities have been made for states in ^{24}Al.

The cross section associated with 1^+ states below an excitation energy of 8 MeV is found in agreement with the large-basis shell-model calculation of Brown and Wildenthal [51]).

Assuming the collective excitations observed around 10 MeV to be a $\Delta L = 1$ resonance with J^π components 0^-, 1^- and 2^-, the expected amount of this strength is exhausted within the rather large experimental errors in estimating the breakup background under the "bump". Similarly most of the $\Delta L = 1$ strength is found to be exhausted in the corresponding region for all investigated self-conjugate nuclei from ^{12}C to ^{40}Ca.

The (^{3}He, t) reaction is found to exhibit a selectivity for exciting the analog of the non-spin-flip giant dipole resonance (GDR), due to its prominent cross section in the first place and on the relatively modest widening of its natural line-shape in the isotopes investigated in this work.

The authors would like to thank H.J. Hofmann and G.W.R. Leibbrandt for their assistance in the data taking and T. Tuintjer for target preparation. We are grateful to P.M. Endt for making the updated tabulation of $A = 24$ levels available to us

before publication. One of us (M.B.G.) wishes to express his gratitude to the staff of the KVI for their kind assistance and continued support and cooperation.

This work was performed as part of the program of the "Stichting Fundamenteel Onderzoek der Materie" (FOM) with support from the "Nederlandse Organisatie voor Wetenschappelijk Onderzoek" (NWO).

References

1) J.D. Anderson and C. Wong, Phys. Rev. Lett. **7** (1961) 250
2) J.D. Anderson, C. Wong and J.W. McClure, Phys. Rev. **126** (1962) 2170
3) J.D. Fox, C.F. Moore and D. Robson, Phys. Rev. Lett. **12** (1964) 198
4) H.J. Kim and R.L. Robinson, Proc. Conf. on Isobaric spin in nuclear physics", ed. J.D. Fox and D. Robson (Academic Press, New York, 1966) p. 487
5) A.G. Blair and H.E. Wegner, Phys. Rev. Lett. **9** (1962) 168
6) R.R. Doering, A. Galonsky, D.L. Patterson and G.F. Bertsch, Phys. Rev. Lett. **35** (1975) 1691
7) C.D. Goodman, C.A. Goulding, M.B. Greenfield, J. Rapaport, D.E. Bainum, C.C. Foster, W.G. Love and F. Petrovich, Phys. Rev. Lett. **44** (1980) 1755
8) C.D. Goodman, C.C. Foster, D.E. Bainum, S.D. Bloom, C. Gaarde, J.S. Larsen, C.A. Goulding, D.J. Horen, T. Masterson, S. Grimes, J. Rapaport, T.N. Taddeucci and E. Sugarbaker, Phys. Lett. **B107** (1981) 406
9) C. Gaarde, J. Rapaport, T.N. Taddeucci, C.D. Goodman, C.C. Foster, D.E. Bainum, C.A. Goulding, M.B. Greenfield, D.J. Horen and E. Sugarbaker, Nucl. Phys. **A369** (1981) 258
10) C. Gaarde, J.S. Larsen, M.N. Harakeh, S.Y. van der Werf, M. Igarashi and A. Müller-Arnke, Nucl. Phys. **A334** (1980) 248
11) D.E. Bainum, J. Rapaport, C.D. Goodman, D.J. Horen, C.C. Foster, M.B. Greenfield and C.A. Goulding, Phys. Rev. Lett. **44** (1980) 1751
12) W.A. Sterrenburg, S.M. Austin, R.P. DeVito and A. Galonsky, Phys. Rev. Lett. **45** (1980) 1839
13) D. Horen, C.D. Goodman, D.E. Bainum, C.C. Foster, C. Gaarde, C.A. Goulding, M.B. Greenfield, J. Rapaport, T.N. Taddeucci, E. Sugarbaker, T. Masterson, S.M. Austin, A. Galonsky and W. Sterrenburg, Phys. Lett. **B99** (1981) 383
14) S.L. Tabor, C.C. Chang, M.T. Collins, G.J. Wagner, J.R. Wu, D.W. Halderson and F. Petrovich, Phys. Rev. **C25** (1982) 1253
15) S.L. Tabor, G. Neuschaefer, J.A. Carr, F. Petrovich, C.C. Chang, A. Guterman, M.T. Collins, D.L. Friesel, C. Glover, S.Y. van der Werf and S. Raman, Nucl. Phys. **A422** (1984) 12
16) W.A. Sterrenburg, M.N. Harakeh, S.Y. van der Werf and A. van der Woude, Nucl. Phys. **A405** (1983) 109
17) W.A. Sterrenburg, S. Brandenburg, J.H. van Dijk, A.G. Drentje, M.B. Greenfield, M.N. Harakeh, H. Riezebos, H. Sakai, W. Segeth, S.Y. van der Werf and A. van der Woude, Nucl. Phys. **A420** (1984) 257
18) S.Y. van der Werf, S. Brandenburg, A.G. Drentje, P. Grasdijk, M.B. Greenfield, M.N. Harakeh, W. Segeth, W.A. Sterrenburg and A. van der Woude, Proc. Int. Symp. on Highly excited states and nuclear structure, Orsay, France, J. de Phys. **45** (1984) C4-471
19) N. Auerbach and A. Klein, Phys. Rev. **C30** (1984) 1032; **C27** (1983) 1818; **C28** (1983) 2075; Nucl. Phys. **A395** (1983) 77
20) G. Bertsch, P.F. Bortignon and R.A. Broglia, Rev. Mod. Phys. **55** (1983) 287
21) S.M. Austin, E. Adamides, A. Galonsky, T. Nees, W.A. Sterrenburg, D.E. Bainum, J. Rapaport, E. Sugarbaker, C.C. Foster, C.D. Goodman, D.J. Horen, C.A. Goulding and M.B. Greenfield, Phys. Rev. Lett., to be submitted.
22) P.D. Kunz, Proc. 1983 RCNP Int. Symp. on Light ion reaction mechanism, Osaka, Japan (1983) p. 304
23) S.Y. van der Werf, S. Brandenburg, P. Grasdijk, W.A. Sterrenburg, M.N. Harakeh, M.B. Greenfield, B.A. Brown and M. Fujiwara, Nucl. Phys. **A496** (1989) 305;
S.Y. van der Werf, 6th Nordic Meeting on nuclear physics, Kopervik, Norway, 1989; Phys. Scr. **T32** (1990) 43

24) J. Rapaport, T.N. Taddeucci, C. Gaarde, C.D. Goodman, C.C. Foster, C.A. Goulding, D. Horen, E. Sugarbaker, T.G. Masterson and D. Lind, Phys. Rev. **C24** (1981) 335
25) C. Gaarde, J.S. Larsen, H. Sagawa, N. Ohtsuka, J. Rapaport, T.N. Taddeucci, C.D. Goodman, C.C. Foster, C.A. Goulding, D. Horen, T. Masterson and E. Sugarbaker, Nucl. Phys. **A422** (1984) 189
26) B.D. Anderson, R.J. McCarthy, M. Ahmad, A. Fazely, A.M. Kalenda, J.N. Knudson, J.W. Watson, R. Madey and C.C. Foster, Phys. Rev. **C26** (1982) 26
27) W. Knüpfer, M. Dillig and A. Richter, Phys. Lett. **B95** (1980) 349
28) A. Richter, Nucl. Phys. **A374** (1982) 177
29) C. Djalali, N. Marty, M. Morlet, A. Willis, J.C. Jourdain, N. Anantaraman, G.M. Crawley and A. Galonski, Nucl. Phys. **A338** (1982) 1
30) G.M. Crawley, N. Anantaraman, A. Galonsky, C. Djalali, N. Marty, M. Morlet, A. Willis, J.-C. Jourdain and P. Kitching, Phys. Rev. **C26** (1982) 87
31) G.M. Crawley, N. Anantaraman, A. Galonsky, C. Djalali, N. Marty, M. Morlet, A. Willis and J.-C. Jourdain, Phys. Lett. **B127** (1983) 322
32) N. Anantaraman, B.A. Brown, G.M. Crawley, A. Galonsky, C. Djalali, N. Marty, M. Morlet, A. Willis, J.C. Jourdain and B.H. Wildenthal, Phys. Rev. Lett. **52** (1984) 1409
33) B.A. Brown and B.H. Wildenthal, At. Data Nucl. Data Tables **33** (1985) 347
34) B.A. Brown and B.H. Wildenthal, Nucl. Phys. **A474** (1987) 290
35) I.S. Towner, Phys. Reports **155** (1987) 264
36) A. Arima, K. Shimizu, W. Bentz and H. Hyuga, Adv. Nucl. Phys. **18** (1987) 1
37) R. Schaeffer, Nucl. Phys. **A158** (1970) 321
38) F. Petrovich and W.G. Love, Nucl. Phys. **A354** (1981) 499c
39) W.G. Love, in The (p, n) reaction and the nucleon-nucleon force, ed. C.D. Goodman, S.M. Austin, S.D. Bloom, J. Rapaport and G.R. Satchler (Plenum, New York, 1980) p. 23
40) W.G. Love and M.A. Franey, Phys. Rev. **C24** (1981) 1073
41) A.G. Drentje, H.A. Enge and S.B. Kowalski, Nucl. Instr. Meth. **122** (1974) 485
42) A.G. Drentje, R.J. de Meijer, H.A. Enge and S.B. Kowalski, Nucl. Instr. Meth. **133** (1976) 209
43) J. van der Plicht and J.C. Vermeulen, Nucl. Instr. Meth. **156** (1978) 103
44) J.C. Vermeulen, J. van der Plicht, A.G. Drentje, L.W. Put and J. van Driel, Nucl. Instr. Meth. **180** (1982) 93
45) P.A. Kroon, Program PAX, unpublished
46) S.C. Fultz, R.A. Alvarez, B.L. Berman, M.A. Kelly, D.R. Lasher and T.W. Phillips, Phys. Rev. **C4** (1971) 149
47) B.L. Berman and S.C. Fultz, Rev. Mod. Phys. **47** (1975) 713
48) J. Raynal, program DWBA82, extended version of DWBA70 (R. Schaeffer and J. Raynal, unpublished)
49) J.R. Comfort, Program DW81, updated 1983, extended version of DWBA70 (R. Schaeffer and J. Raynal, unpublished)
50) R. Schaeffer and J. Raynal, Program DWBA70, unpublished
51) B.A. Brown and B.H. Wildenthal, Ann. Rev. Nucl. Part. Sci. **38** (1988) 29;
B.H. Wildenthal, Prog. Part. Nucl. Phys. **11** (1984) 5
52) P. Grasdijk, M.N. Harakeh and S.Y. van der Werf, KVI Annual Report 1985, p. 36;
P. Grasdijk, Thesis, University of Groningen (1986), unpublished
53) P.M. Endt, Nucl. Phys. A521 (1990) 1
54) R.E. Tribble and A.V. Nero, Phys. Rev. **C15** (1977) 2233;
R.J. Peterson, Phys. Rev. **C16** (1977) 2424
55) V. Gillet and N. Vinh Mau, Nucl. Phys. **54** (1964) 321; **57** (1964) 698(E)
56) J.M. Clark and J.P. Elliot, Phys. Lett. **19** (1965) 294
57) U.E.P. Berg, S.M. Austin, R. DeVito, A.I. Galonsky and W.A. Sterrenburg, Phys. Rev. Lett. **45** (1980) 11
58) J. Miller, G. Schuhl, G. Tamas and C. Tzara, Phys. Lett. **2** (1962) 76; J. Phys. **27** (1966) 8
59) E.H.L. Aarts, R.K. Bhowmik, R.J. de Meijer and S.Y. van der Werf, Phys. Lett. **B102** (1981) 307
60) E.H.L. Aarts, R.A.R.L. Malfliet, R.J. de Meijer and S.Y. van der Werf, Nucl. Phys. **A425** (1984) 23
61) J. Speth and A. van der Woude, Rep. Prog. Phys. **44** (1981) 719